International Journal of Pharmaceutics 371 (2009) 142–147

Contents lists available at ScienceDirect

International Journal of Pharmaceutics

journal homepage: www.elsevier.com/locate/ijpharm

Pharmaceutical Nanotechnology

Enhanced electrostatic interaction between chitosan-modified PLGA nanoparticle and tumor

Rui Yang[a,b,c], Won-Sik Shim[a,b], Fu-De Cui[c], Gang Cheng[c], Xu Han[c], Qing-Ri Jin[a,b], Dae-Duk Kim[a], Suk-Jae Chung[a], Chang-Koo Shim[a,b,*]

[a] Research Institute of Pharmaceutical Sciences, College of Pharmacy, Seoul National University, Seoul 151-742, Republic of Korea
[b] National Research Laboratory for Transporters Targeted Drug Design, College of Pharmacy, Seoul National University, Seoul 151-742, Republic of Korea
[c] Department of Pharmaceutics, College of Pharmacy, Shenyang Pharmaceutical University, Shenyang 110016, China

ARTICLE INFO

Article history:
Received 28 August 2008
Received in revised form
10 November 2008
Accepted 4 December 2008
Available online 11 December 2008

Keywords:
PLGA nanoparticles
Chitosan
Paclitaxel
Coumarin 6
Electrostatic interaction
Extracellular tumor pH
Zeta potential
Tumor
Targeting

ABSTRACT

In our previous study, lung tumor-specific targeting of paclitaxel was achieved in mice by intravenous administration of chitosan-modified paclitaxel-loaded PLGA nanoparticles (C-NPs-paclitaxel). Transient formation of aggregates in the blood stream followed by enhanced trapping in the capillaries was proposed as a mechanism of the lung-specific accumulation of paclitaxel. In the present study, the mechanism of tumor lung preferential accumulation of paclitaxel from C-NPs-paclitaxel was investigated. Zeta potential and *in vitro* cellular cytotoxicity (A549 cells and CT-26 cells) of C-NPs-paclitaxel, and *in vitro* uptake of coumarin 6 to these cells from chitosan-modified coumarin 6 containing PLGA nanoparticles (C-NPs-coumarin 6) were examined as a function of pH (6.8, 7.4 and 8.0). The zeta potential of C-NPs-paclitaxel increased as the medium pH became more acidic. *In vitro* uptake of coumarin 6 by A549 cells and CT-26 cells was enhanced at lower pH for C-NPs-coumarin 6. *In vitro* cytotoxicity experiment with C-NPs-paclitaxel demonstrated enhanced cytotoxicity as the pH became more acidic. Therefore, enhanced electrostatic interaction between chitosan-modified PLGA nanoparticles and acidic microenvironment of tumor cells appears to be an underlying mechanism of lung tumor-specific accumulation of paclitaxel from C-NPs-paclitaxel.

1. Introduction

The use of chemotherapy to treat cancers is often limited by unwanted toxic effects on normal tissues. This is because most anti-cancer drugs are not distributed in the target tumor-bearing tissues specifically, which results in reduced therapeutic efficacy. Therefore, it is evident that targeted delivery of anti-cancer drugs into the tumor tissue is the focus of intensive research to improve chemotherapy (Kobayashi and Lin, 2006). For this reason, various drug carriers have been investigated to reduce toxicity and to increase therapeutic efficacy of anti-cancer drugs. However, the attempt is regarded as a limited success, particularly for lung tumors (Lee et al., 2008).

With regard to lung cancers, Taxol® is one of the first line formulations of paclitaxel that can be used in the treatment of non-small cell lung cancer (NSCLS), which has the highest mortality rate among cancers (Parkin et al., 2005). However, Cremophor® EL – an adjuvant used in Taxol® – has been associated with very serious side effects such as hypersensitivity reactions, nephrotoxicity, neurotoxicity, and cardiotoxicity (Lehoczky et al., 2001). Moreover, it has recently been found that the concentration of paclitaxel in the lung is very low (Yang et al., 2008), possibly resulting in unsatisfactory therapeutic efficacy.

To overcome this limitation, we have prepared "chitosan-modified, paclitaxel-loaded poly lactic-co-glycolic acid (PLGA) nanoparticles" (C-NPs-paclitaxel) with a mean diameter of 200–300 nm (Yang et al., 2008). As a result, a lung-specific increase of paclitaxel concentration was achieved in mice using C-NPs-paclitaxel, while "chitosan-unmodified paclitaxel-loaded PLGA nanoparticles" (U-NPs-paclitaxel) did not. Transient formation of aggregates of nanoparticles in the blood stream followed by enhanced trapping in the lung capillaries was proposed as a mechanism of lung tumor-specific distribution of C-NPs-paclitaxel. Moreover, C-NPs-paclitaxel seemed to have an affinity for lung tumor tissues, because the concentration of paclitaxel in the tumor-bearing lung was greater than that in the normal lung. We reasoned that this phenomenon could be due to the electrostatic interaction between nanoparticles and tumor tissues. However,

* Corresponding author at: Research Institute of Pharmaceutical Sciences, College of Pharmacy, Seoul National University, Seoul 151-742, Republic of Korea.
Tel.: +82 2 880 7873; fax: +82 2 888 5969.
E-mail address: shimck@snu.ac.kr (C.-K. Shim).

0378-5173/$ – see front matter © 2009 Published by Elsevier B.V.
doi:10.1016/j.ijpharm.2008.12.007

no conclusive evidence was given in the last study (Yang et al., 2008).

Numerous reports confirm that the extracellular region of various solid tumors is acidic (Adams, 2005). The acidic pH is regarded even as a phenotypic characteristic of tumor growth and invasiveness of solid tumors. Under these acidic conditions, it is known that the surface charges of chitosan-modified nanoparticles become more positive (Nafee et al., 2007). On the other hand, cancer cell membranes are negatively charged (Augustin et al., 1995; Augustin et al., 1994; Iozzo and San-Antonio, 2001; Ran et al., 2002; Ran and Thorpe, 2002; Kirkpatrick et al., 2003). Therefore, a stronger electrostatic interaction between negatively charged tumor vascular cells and positively charged C-NPs is assumed to occur at acidic tumor tissues. In the present study, the underlying mechanism of the lung tumor-specific accumulation of chitosan-modified PLGA nanoparticles was investigated in detail in terms of electrostatic interaction.

2. Materials and methods

2.1. Materials

Paclitaxel was purchased from Taihua National Plant Pharmaceutical Corporation (Shan Xi, China). PLGA with a lactide/glycolide molar ratio of 50:50 (Mw: 40,000–75,000), polyvinyl alcohol (PVA, Mw: ~67,000), chitosan (Mw: 45,500–50,000, deacetylation degree: 75–80%), coumarin 6 (Mw: 350.43), RPMI 1640 cell culture medium (powder with L-glutamine and without sodium bicarbonate, developed at Roswell Park Memorial Institute) and phosphate-buffered saline (PBS, pH 7.4, 0.01 M) were purchased from Sigma–Aldrich (St. Louis, MO, USA). A human lung cancer cell line A549 and the murine colon cancer cell line CT-26 were purchased from Korea Cell Line Bank (Seoul, Korea). All other chemicals were of the highest grade available and were obtained from commercial sources.

2.2. Animals and induction of lung tumor

Male CDF_1 mice, 3–4 weeks old and weighting 18–22 g, were purchased from the Central Lab Animal Inc. (Seoul, Korea). A transplantable mouse colon cancer cell line (CT-26), which was maintained in RPMI 1640 medium supplemented with 10% FBS, 100 IU/mL penicillin, 100 μg/mL streptomycin, and 2 mM L-glutamine in 5% CO_2 humidified air at 37 °C, was administered to the CDF_1 mice via the tail vein at a concentration of 1×10^5 cells/mouse. Exactly 2 weeks after the injection of CT-26 cells, the animals were used as lung tumor-bearing mice (Sakurai et al., 2003). All animal experiments were performed according to the Guidelines for Animal Care and Use of Seoul National University, Seoul, Korea.

2.3. Preparation of PLGA nanoparticles

Paclitaxel- or coumarin 6-loaded PLGA nanoparticles were prepared as described previously (Yang et al., 2008). Briefly, PLGA and either paclitaxel or coumarin 6 were dissolved in dichloromethane, poured into a PVA solution (4%, w/v) and sonicated. The resulting o/w pre-emulsion was poured into a larger volume of PVA solution (1%, w/v) in order to increase the distance between emulsified droplets and to minimize coalescence and aggregation of the newly formed particles being formed. The dispersion was stirred overnight at 40 °C, centrifuged at 919.7 × *g* and then at 41,137.3 × *g* to separate the particles. The resulting sediments were resuspended in double distilled water. This process was repeated three times. In the case of chitosan-modified nanoparticles, either paclitaxel- or coumarin 6-loaded nanoparticles was added to the chitosan acetic acid solution (1%, v/v) under agitation with a magnetic stirrer overnight at room temperature. Subsequently, the mixture was centrifuged at 92,566.5 × *g* for 50 min, and the unbounded polymer in the supernatant was decanted. Finally, the resulting dispersion was freeze-dried. The chitosan modification did not influence the content of the drug in the nanoparticles (*e.g.*, paclitaxel in C-NPs-paclitaxel and U-NPs-paclitaxel was identical at 3.41 ± 0.12% (w/w); coumarin 6 in C-NPs-coumarin 6 and U-NPs-coumarin 6 was identical at 3.58 ± 0.16 (w/w)). The sizes of C-NPs-paclitaxel or C-NPs-coumarin 6 were 281 ± 3.61 nm or 279 ± 3.69 nm (mean ± S.D., $n = 3$), respectively, while those of U-NPs-paclitaxel or U-NPs-coumarin 6 were 202 ± 2.34 nm or 205 ± 3.76 nm (mean ± S.D., $n = 3$), respectively.

2.4. Zeta potential of nanoparticles at various pH

The surface charge of the chitosan-modified (C-NPs) or unmodified nanoparticles (U-NPs) was measured by electrophoretic light scattering spectrophotometry (ELS-8000, Otsuka Electronics Co. Ltd., Osaka, Japan), based on dynamic light scattering, after appropriate dilution of the nanoparticles in PBS solution of different pH values (pH 5.5–8.0).

2.5. In vitro cell uptake of coumarin 6 from C-NPs-coumarin 6 or U-NPs-coumarin 6 at different pH

To examine the effect of surface modification with chitosan on the cellular uptake of nanoparticles at different pH, an *in vitro* uptake experiment was performed for U-NPs-coumarin 6 and C-NPs-coumarin 6 using A549 and CT-26 cells. The cells were routinely grown at 37 °C with an RPMI 1640 medium, supplemented with 10% fetal bovine serum (FBS), 100 IU/mL penicillin, 100 μg/mL streptomycin and 2 mM L-glutamine (both from Welgene Inc. Daegu, Korea) in a 5% CO_2/95% air humidified atmosphere. A549 or CT-26 cells were seeded into 96-well microplates (Black Clear Bottom Cell Culture Microplates 3603, Corning Costar Corp., Cambridge, MA, USA) at a cellular density of 1×10^4 cells/well. When the cells reached 80% confluence, the medium was replaced with 100 μL PBS buffer of various pHs (6.8, 7.4 and 8.0), containing coumarin 6-loaded PLGA nanoparticles (0.25 mg/mL). Coumarin 6 was selected as a model compound based on its high sensitivity of determination in the cell. The plates were incubated for 6 h or 12 h at 37 °C. The incubation was terminated by the addition of ice-cold PBS (100 μL), and the PBS was removed. This process was repeated twice to eliminate nanoparticles that were not taken up by the cells. The cell membrane was then lysed with 100 μL of 0.5% triton X-100 solution in 0.2 N NaOH, and the concentration of coumarin 6 in the lysate was determined using a microplate reader (Synergy HT, BioTek Instruments, Winooski, VT, USA) at excitation and emission wavelengths of 430 and 485 nm, respectively.

2.6. In vitro cell cytotoxicty of C-NPs-paclitaxel and U-NPs-paclitaxel

A549 or CT-26 cells were transferred to 96-well plates (Corning Costar Corp, New York, USA) at a density of 1×10^4 cells/well. When the cells reached 80% confluence, the medium was replaced with 100 μL of medium at a pH of 6.8, 7.4 or 8.0 containing varying amounts of U-NPs-paclitaxel or C-NPs-paclitaxel. One row of the 96-well plates was used as a control; culture medium without the nanoparticles was added to these wells. The plates were then incubated for 6 h or 12 h. The medium was then removed and the wells were washed three times with PBS (100 μL). Then, 100 μL of 3-(4,5-dimethylthiazol-2-yi)-2,5-diphenyltetrazolium (MTT assay solution), which was prepared by mixing 10 μL of MTT stock solution (5 mg/mL) and 90 μL of incubation medium, respectively,

was added to each well, followed by a 3 h incubation period. After incubation, the medium was removed, and dimethylsulfoxide (DMSO, 100 μL) was added to the residual precipitates. The absorbance of the resulting DMSO solution was determined at 560 nm using a microplate reader (Molecular Devices Co., Sunnyvale, CA). Cell viability was expressed as the percent absorbance relative to absorbance measured for cells that were not exposed to any material. Relative absorbance was plotted against the log (drug concentration) for the determination of the nanoparticles concentration that resulted in 50% cytotoxicity (IC_{50}) value. IC_{50} and 95% confidence intervals were calculated using non-linear regression of log-transformed data by Prism (Graph Pad software, San Diego, CA) (Banfi et al., 2007).

2.7. Confocal laser scanning microscopy

A549 and CT-26 cells were seeded onto 6-well glass inserts (3516, Corning Costar Corp., MA, USA) at a cellular density of 5×10^5 cells/well. When 80% confluence was reached, the culture medium was replaced with 1 mL medium (pH 6.8, 7.4 or 8.0) containing U-NPs-coumarin 6 or C-NPs-coumarin 6 (0.25 mg/mL). After incubation at 37 °C for 6 h, the medium was removed by aspiration, and the cells were rinsed three times with ice-cold PBS (1 mL) and fixed with 3.7% formaldehyde (0.5 mL). Thereafter, glass inserts containing the cells were observed under confocal laser scanning microscopy (TCS SP2, Leica Microsystem, Heidelberg GmbH, Mannheim, Germany) after mounting by the reagent (FluoSave, Calbiochem, San Diego, CA, USA). The intensity of the brightness was analysed using Image J (National Institutes of Health, Maryland, USA).

To investigate the distribution profile of C-NPs-coumarin 6 *in vivo*, the nanoparticles were administered to mice via the tail vein at a coumarin 6 dose of 10 mg/kg. Lungs were carefully harvested 2 h after the administration of the nanoparticles, fixed and preserved in 10% neutral buffered formalin (~ 4% formalin solution). Organs were then trimmed, embedded in paraffin, and cut into ~2 μm sections. Thereafter, lung tissues slices were directly placed in a sample holder, covered with a coverslip glass, and observed under confocal laser scanning microscopy (TCS SP2, Leica Microsystem, Heidelberg GmbH, Mannheim, Germany) (Lombry et al., 2002).

2.8. Statistical analysis

Data were analysed for statistical significance by one-way analysis of variance (ANOVA) followed by Sheffe's test. Either $p < 0.001$ or $p < 0.05$ was considered as statistically significant.

3. Results and discussion

3.1. Zeta potential of C-NPs-paclitaxel and U-NPs-paclitaxel at various pH

First, it was investigated whether surface charges of nanoparticles are affected by various medium conditions. As shown in Fig. 1, the zeta potentials of C-NPs-paclitaxel became higher as the medium became more acidic. For instance, the positive potential at pH 5.5 was approximately 20-fold greater than that at pH 8.0 (*e.g.*, 41.4 mV at pH 5.5 vs. 2.09 mV at pH 8.0). On the contrary, the zeta potentials of U-NPs-paclitaxel were not significantly influenced by the pH.

Chitosan is poly-cationic in acidic media and thus the zeta potential increases as the medium becomes more acidic (Khunawattanakul et al., 2008). This phenomenon might be due to the presence of free amines on chitosan molecules. In particular, the amino group ($-NH_2$) forms a cationic amine group ($-NH_3^+$)

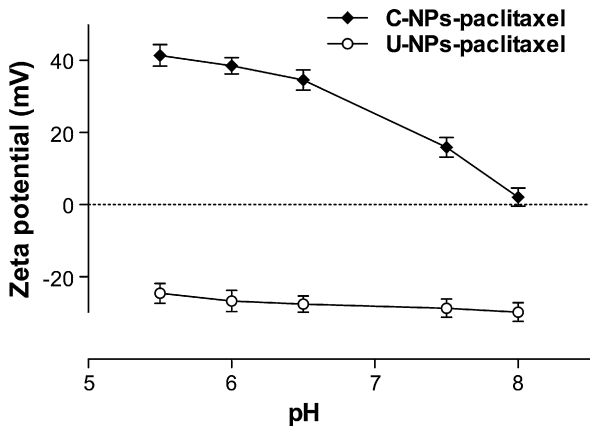

Fig. 1. Zeta potential (mV) of chitosan-modified paclitaxel-loaded PLGA nanoparticles (C-NPs-paclitaxel) and unmodified paclitaxel-loaded PLGA nanoparticles (U-NPs-paclitaxel) in various pH PBS solution.

in an acidic environment. The following equilibrium describes the state of ionization:

$$\text{Chit-NH}_2 + \text{H}_3\text{O}^+ \leftrightarrow \text{Chit-NH}_3^+ + \text{H}_2\text{O}$$

Therefore, pH is an important parameter for C-NPs because it affects not only the ionization of chitosan molecules, but also the zeta potential of C-NPs. As the pH of the medium increased (*e.g.*, at pH 8.0), the zeta potential decreased, probably due to a reduction in ionization of the amine group. In comparison, the negative charge of U-NPs was attributable to the presence of polymeric carboxylic groups on the surface of PLGA nanoparticles (Lacasse et al., 1998; Mauduit and Vert, 1993). It appears that the surface charges of U-NPs are not affected by the pH difference, because the zeta potential changes were negligible (Fig. 1). It is worth mentioning that the zeta potential changes of U-NPs were only 0.4–3.5 mV for the conditions of pH 2.0–8.0 (Nafee et al., 2007).

In short, the zeta potential of C-NPs, but not that of U-NPs, was greatly affected by the pH, indicating that C-NPs will be more positively charged under acidic conditions.

3.2. In vitro cell uptake of coumarin 6 from C-NPs-coumarin 6 and U-NPs-coumarin 6

The effect of pH on the cellular uptake of coumarin 6 was then examined for A549 and CT-26 cells. As shown in Fig. 2, the fluorescence intensities from C-NPs-coumarin 6 for a 6 h period for both cell lines were greater than those of U-NPs-coumarin 6. In addition, the fluorescence intensities of C-NPs from both A549 and CT-26 cells became stronger as the pH of the medium became acidic, indicating that the uptake of C-NPs were more active under acidic conditions (*i.e.*, pH 6.8 > pH 7.4 > pH 8.0). On the other hand, the intensities of U-NPs showed no noticeable changes, suggesting that the uptake process of U-NPs is pH-insensitive. Most of the uptake in Fig. 2 could be attributable to the uptake of nanoparticles rather than the uptake of released coumarin 6 because the release of coumarin 6 during the 6 h period was minimal (*i.e.*, <5%, regardless of pH, under the given conditions, data not shown).

The uptake amount of coumarin 6 by both cell lines was further quantified for more exact comparison. Fig. 3 shows the quantified amounts of coumarin 6 under various pH conditions. In line with confocal microscopy results (Fig. 2), cellular uptake of C-NPs was much greater compared with U-NPs at all pHs examined, and increased significantly as the pH in the medium decreased for both cell lines. However, the uptake of U-NPs was not affected by the pH change ($0.21–0.41 \times 10^{-10}$ mmol/cm^2). Again, most of the uptake in Fig. 3 could be attributable to the uptake of nanoparticles rather

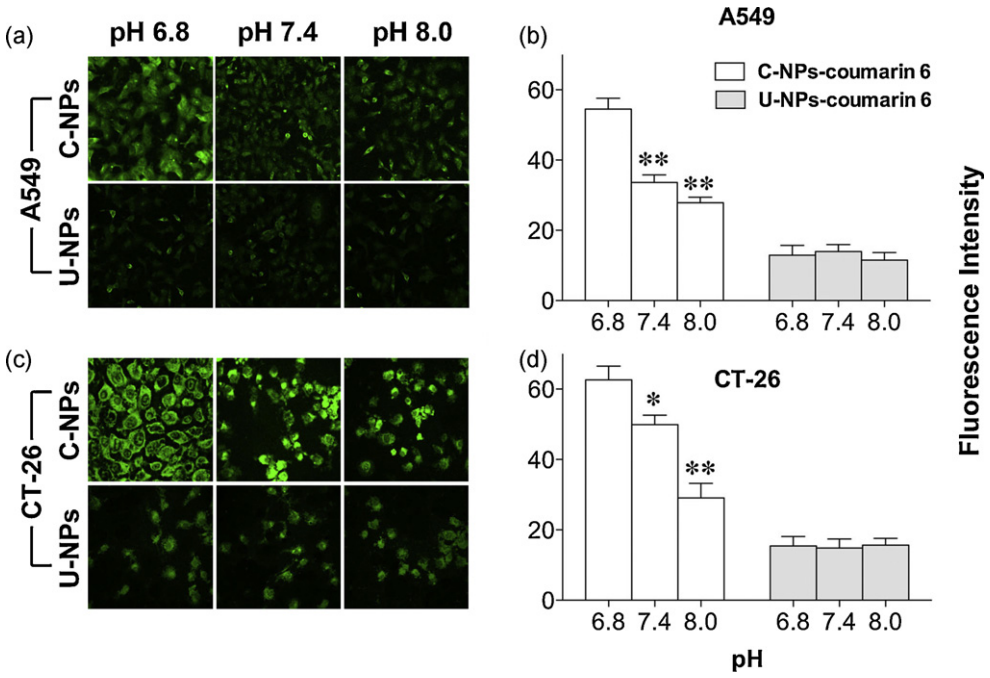

Fig. 2. Representative confocal microscopic images of A549 (a) and CT-26 cells (c) following incubation for 6 h with chitosan-modified coumarin 6-loaded PLGA nanoparticles (C-NPs-coumarin 6) and unmodified coumarin 6-loaded PLGA nanoparticles (U-NPs-coumarin 6) at pH 6.8, 7.4 or 8.0. The fluorescence intensities of A549 (b) and CT 26 cells (d) are shown as graphs ($n = 3$). $^{*}P < 0.05$, $^{**}P < 0.001$.

than the uptake of released coumarin 6 because the release of coumarin 6 during the 12 h period was minimal (*i.e.*, <8%, regardless of pH, under the given conditions, data not shown).

The positive charge (zeta potential) on C-NPs is enhanced at lower pH, as demonstrated in Fig. 1. Cell surfaces, especially cancer cell surfaces, are usually charged negatively due to the translocation of negatively charged constituents of the inner layer of the cell membrane (*e.g.*, phosphatidylserine, anionic phospholipids, glycoproteins and proteoglycans) to the cell surfaces in the case of cancers (Augustin et al., 1994, 1995; Iozzo and San-Antonio, 2001; Ran et al., 2002; Ran and Thorpe, 2002; Kirkpatrick et al., 2003). The increased uptake of C-NPs into the cell at lower pH medium, therefore, appears to be attributable in part to the electrostatic interaction between the positive charge of C-NPs and negative charge of the cancer cell surfaces.

3.3. *In vitro cytotoxicity of C-NPs-paclitaxel and U-NPs-paclitaxel*

Next, whether the pH affects the cytotoxicity of C-NPs-paclitaxel and U-NPs-paclitaxel was tested. The cytotoxicity in the culture

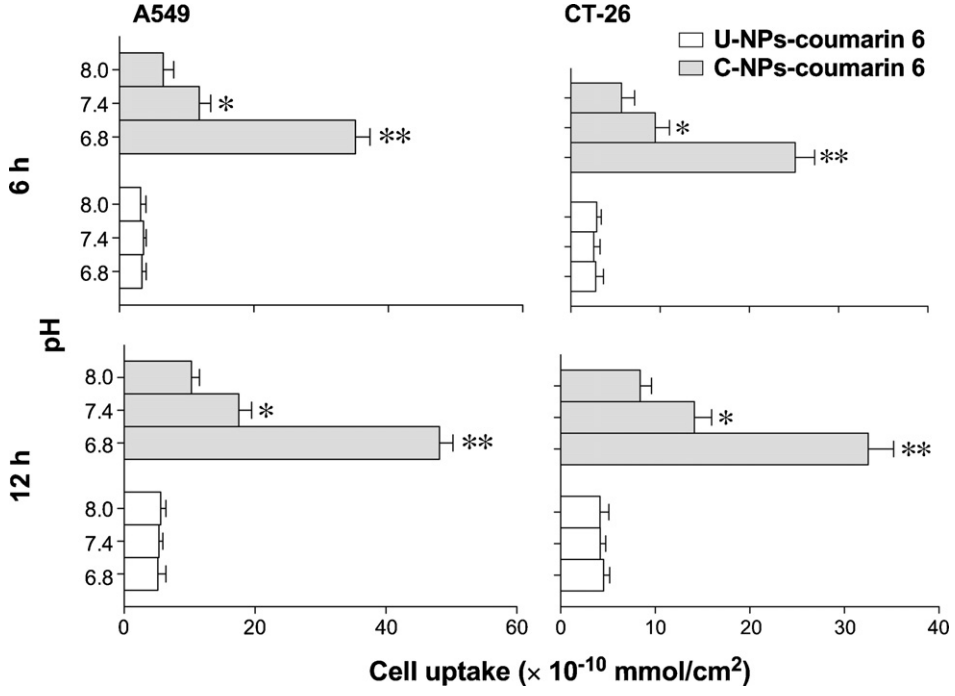

Fig. 3. Cellular uptake of C-NPs-coumarin 6 and U-NPs-coumarin 6 in A549 and CT-26 cells under various pH PBS after 6 and 12 h of incubation ($n = 3$). $^{*}P < 0.05$, $^{**}P < 0.001$.

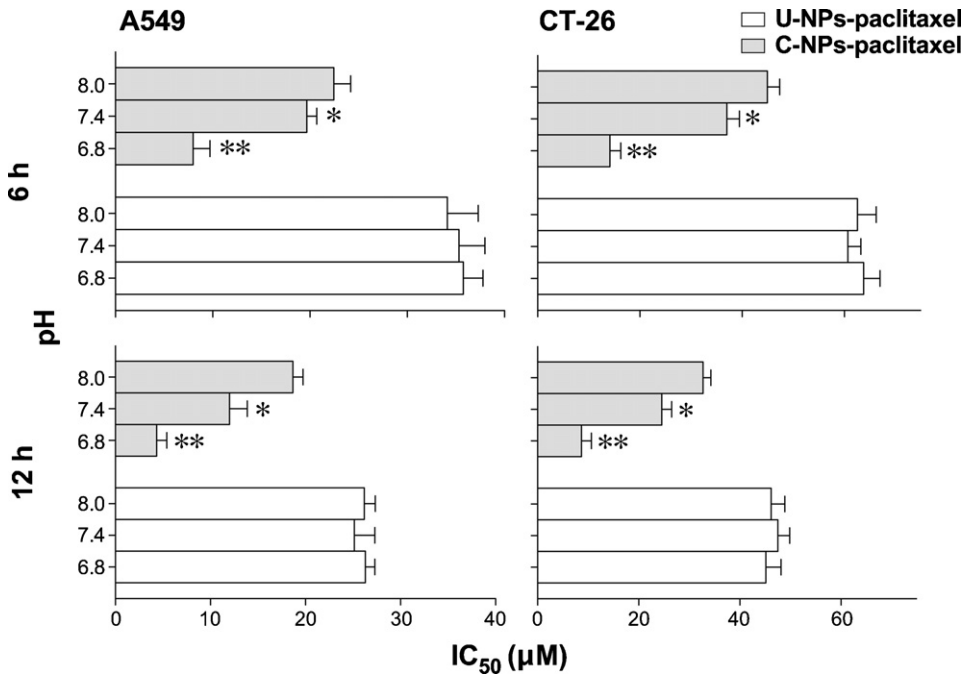

Fig. 4. Cytotoxicity of paclitaxel-loaded C-NPs and U-NPs in various pH values against A549 and CT-26 cells after 6 and 12 h of incubation ($n = 3$). $^{*}P < 0.05$, $^{**}P < 0.001$.

medium of different pH values was evaluated by comparing IC_{50} values from both A549 cells and CT-26 cells. As shown in Fig. 4, the IC_{50} of C-NPs decreased in both cell lines as the cell culture medium became more acidic. For example, IC_{50} values in A549 cells decreased from 18.68 ± 1.06 to 4.35 ± 0.71 μM as the pH of the medium changed from 8.0 to 6.8 during the 12 h incubation. A similar result was observed for CT-26 cells, but IC_{50} values of CT-26 cells were higher than those of A549 cells. On the other hand, U-NPs exerted constant IC_{50} values regardless of the pH of the medium. After the 12 h incubation, greater sensitivity was observed compared with 6 h incubation for both cells and nanoparticles (Fig. 4).

Because paclitaxel itself is not a pH-sensitive cancer chemotherapeutic agent (Fitzpatrick and Wheeler, 2003), and the release of paclitaxel to medium in any pH is less than 10% (data not shown), greater sensitivity to C-NPs at lower pH might be due to the enhanced interaction between the positive nanoparticles (*i.e.*, C-NPs) and negative cancer cells. As previously mentioned, more positive charges on C-NPs at lower pH and greater negative charges of the cancer cell membrane might have induced the electrostatic interaction between nanoparticles and cell membranes, enhancing the uptake of nanoparticles into cells, and the cytotoxic effects of paclitaxel against the cancer cells.

3.4. Tumor-specific accumulation of C-NPs in vivo

Finally, whether C-NPs are specifically accumulated in lung cancers *in vivo* was checked microscopically. C-NPs-coumarin 6 was injected intravenously into both normal and lung tumor-bearing mice at a coumarin 6 dose of 10 mg/kg. As shown in Fig. 5, the accumulation of coumarin 6 in the tumor tissue 2 h after administration was greater than that observed in the normal tissue, which is con-

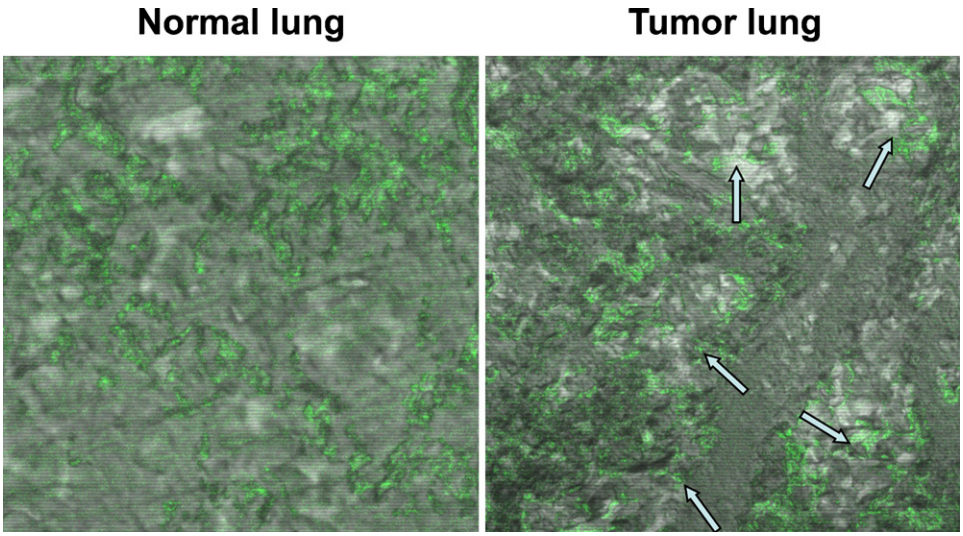

Fig. 5. A representative distribution of coumarin 6-loaded C-NPs in the lung tissue 2 h after tail vein administration at a coumarin 6 dose of 10 mg/kg. The green staining represents coumarin 6-labeled nanoparticles in normal lung (left) and tumor lung (right). Arrows indicate the tumor nodules. Magnification was 512×.

sistent with a greater distribution index (*i.e.*, AUC_{lung}/AUC_{plasma}) of paclitaxel in the lung for tumor-bearing mice compared to normal mice (*i.e.*, 99.9 vs. 71.9, Yang et al., 2008).

The tumor-specific accumulation of drugs could be achieved by the electronic interaction between cationic drug delivery systems and anionic tumor microvessels (Schmitt-Sody et al., 2003). In the present study, the acidic microenvironment of the tumor site might have increased the positive charges on the surface of C-NPs-coumarin 6, thereby enhancing the electrostatic interaction between the nanoparticles and the tumor cells.

Evidence accumulated during the past 50 years shows that the pH of most solid tumors in patients ranges from 5.7 to 7.8 with a mean value of 7.0. Moreover, greater than 80% of these measured values are smaller than pH 7.2 (Lee et al., 2003). Tumor tissues contain large, acid-outside plasma pH gradients, while normal tissues generally have alkaline-outside pH gradients (Mahoney et al., 2003). Therefore, the extracellular pH of malignant tumors is significantly lower than that of normal tissues under physiological conditions (Gerwek, 1998, 2000; Garcia-Martin et al., 2006). As the pH became acidic, the zeta potential of V-NPs became positive (Fig. 1), which enhanced the electrostatic interaction between the C-NPs and tumor tissues. In addition, negative charges on the endothelial cell membranes of the tumor vasculature might have potentiated the electrostatic interaction between positively charged nanoparticles and tumors. Thus, these two factors – more positive charges of C-NPs at the tumor site and more negative charges of tumor cells/vasculature – appear to be responsible for the tumor-specific accumulation of C-NPs.

In conclusion, accelerated *in vitro* uptake of coumarin 6 to cancer cells (Figs. 2 and 3), enhanced cytotoxicity of paclitaxel (Fig. 4) and increased *in vivo* accumulation of coumarin 6 in tumor-bearing lungs (Fig. 5) consistently suggest that enhanced electrostatic interaction between nanoparticles and tumor tissues serves as an underlying mechanism for the lung tumor-specific sensitivity of chitosan-modified nanoparticles. This novel mechanism of the C-NP delivery system may bring us a step closer to a safe and universal targeting system for acidic solid tumors.

Acknowledgements

This study was supported by a grant from the Korean Science and Engineering Foundation (KOSEF) through the National Research Laboratory Program founded by the Ministry of Science and Technology (ROA-2006-000-10290-0).

References

Adams, D.J., 2005. The impact of tumor physiology on camptothecin-based drug development. Curr. Med. Chem. Anticancer Agents 5, 1–13.
Augustin, H.G., Braun, K., Telemenakis, I., Modlich, U., Kuhn, W., 1995. Ovarian angiogenesis phenotypic characterization of endothelial cells in a physiological model of blood vessel growth and regression. Am. J. Pathol. 147, 339–351.
Augustin, H.G., Kozian, D.H., Johnson, R.C., 1994. Differentiation of endothelial cells: analysis of the constitutive and activated endothelial cell phenotypes. Bioassays 16, 901–906.
Banfi, S., Caruso, E., Buccafurni, L., Ravizza, R., Gariboldi, M., Monti, E., 2007. Zinc phthalocyanines-mediated photodynamic therapy induces cell death in adenocarcinoma cells. J. Organomet. Chem. 692, 1269–1276.
Fitzpatrick, F.A., Wheeler, R., 2003. The immunopharmacology of paclitaxel (Taxol®), docetaxel (Taxotere®), and related agents. Int. Immunopharmacol. 3, 1699–1714.
Garcia-Martin, M.L., Martinez, G.V., Raghunand, N., Sherry, A.D., Zhang, S., Gillies, R.J., 2006. High resolution pHe imaging of rat glioma using pH-dependent relaxivity. Magn. Reson. Med. 55, 309–315.
Gerwek, L.E., 1998. Tumor pH: implications for treatment and novel drug design. Semin. Radiat. Oncol. 8, 176–182.
Gerwek, L.E., 2000. The pH difference between tumor and normal tissue offers a tumor specific target for the treatment of cancer. Drug Resist. Update 3, 49–50.
Iozzo, R.V., San-Antonio, J.D., 2001. Heparan sulfate proteoglycans: heavy hitters in the angiogenesis arena. J. Clin. Invest. 108, 349–355.
Khunawattanakul, W., Puttipipatkhachorn, S., Rades, T., Pongjanyakul, T., 2008. Chitosan–magnesium aluminum silicate composite dispersions: characterization of rheology, flocculate size and zeta potential. Int. J. Pharm. 351, 227–235.
Kirkpatrick, A.P., Kaiser, T.A., Shepherd, R.D., Rinker, K.D., 2003. Biochemical mediated glycocalyx modulation in human umbilical vein endothelial cells (HUVEC). Summer Bioeng. Conf., 25–29.
Kobayashi, T., Lin, P.C., 2006. Nanotechnology for antiangiogenic cancer therapy. Nanomedicine 1, 17–22.
Lacasse, F.X., Filion, M.C., Phillips, N.C., Escher, E., McMullen, J.N., Hildgen, P., 1998. Influence of surface properties at biodegradable microsphere surfaces: effects on plasma protein adsorption and phagocytosis. Pharm. Res. 15, 312–317.
Lee, E.S., Na, K., Bae, Y.H., 2003. Polymeric micelle for tumor pH and folate-mediated targeting. J. Control Release. 91, 103–113.
Lee, J.M., Yanagawa, J., Peebles, K.A., Sharma, S., Mao, J.T., Dubinett, S.M., 2008. Inflammation in lung carcinogenesis: new targets for lung cancer chemoprevention and treatment. Crit. Rev. Oncol. Hematol. 66, 208–217.
Lehoczky, O., Bagaméri, A., Udvary, J., Pulay, T., 2001. Side-effects of paclitaxel therapy in ovarian cancer patents. Eur. J. Gynaecol. Oncol. 22, 81–84.
Lombry, C., Bosquillon, C., Préat, V., Vanbever, R., 2002. Confocal imaging of rat lungs following intratracheal delivery of dry powders or solutions of fluorescent probes. J. Control Release 83, 331–341.
Mahoney, B.P., Raghunand, N., Baggett, B., Gillies, R.J., 2003. Tumor acidity, ion trapping and chemotherapeutics. I. Acid pH affects the distribution of chemotherapeutic agents in vitro. Biochem. Pharmacol. 66, 1207–1218.
Mauduit, J., Vert, M., 1993. Poly(lactic acid)/poly(glycolic acid) homo- and copolymers and sustained drug delivery. S.T.P. Pharma Sci. 3, 197–212.
Nafee, N., Taetz, S., Schneider, M., Schaefer, U.F., Lehr, C.M., 2007. Chitosan-coated PLGA nanoparticles for DNA/RNA delivery: effect of the formulation parameters on complexation and transfection of antisense oligonucleotides. Nanomedicine 3, 173–183.
Parkin, D.M., Bray, F., Ferlay, J., Pisani, P., 2005. Global cancer statistics. CA Cancer J. Clin. 55, 74–108.
Ran, S., Downes, A., Thorpe, P.E., 2002. Increased exposure of anionic phospholipids on the surface of tumor blood vessels. Cancer Res. 62, 6132–6140.
Ran, S., Thorpe, P.E., 2002. Phosphatidylserine is a marker of tumor vasculature and a potential target for cancer imaging and therapy. Int. J. Radiat. Oncol. Biol. Phys. 54, 1479–1484.
Sakurai, F., Terada, T., Maruyama, M., Watanabe, Y., Yamashita, F., Takakura, Y., Hashida, M., 2003. Therapeutic effect of intravenous delivery of lipoplexes containing the interferon-β gene and poly I: poly C in a murine lung metastasis model. Cancer Gene Ther. 10, 661–668.
Schmitt-Sody, M., Strieth, S., Krasnici, S., Sauer, B., Schulze, B., Teifel, M., Michaelis, U., Naujoks, K., Dellian, M., 2003. Neovascular targeting therapy: paclitaxel encapsulated in cationic liposomes improves antitumoral efficacy. Clin. Cancer Res. 9, 2335–2341.
Yang, R., Yang, S.G., Shim, W.S., Cui, F., Chang, G., Kim, I.W., Kim, D.D., Chung, S.J., Shim, C.K., 2008. Lung-specific delivery of paclitaxel by chitosan-modified PLGA nanoparticles via transient formation of microaggregates. J. Pharm. Sci. 98, 970–984.